JOURNAL OF MATERIALS SCIENCE 26 (1991) 3874–3878

$Ni(Al, Fe)_2O_4$–TiO_2 ceramic humidity sensors

LONG WU, CHEN-CHENG WU, JEN-CHENG HER
Department of Electrical Engineering, National Cheng Kung University, Tainan, Taiwan

In this study, the electrical resistance relative to the water absorption of humidity sensors made from $Ni(Al, Fe)_2O_4$–TiO_2 ceramic is investigated. This ceramic body forms a spinel structure after sintering and exhibits a porous structure. Porous ceramics easily absorb and desorb water vapour through the pores, and the electrical conductivity is enhanced by water absorption. In this ceramic system the conduction mechanism is ionic. The $Ni(Al, Fe)_2O_4$–TiO_2 porous ceramic has a high humidity activity, short response time for humidity detection (less than 40 s), and high stability. The highest sensitivity among the specimens studied is found in $Ni(Al_{0.875}Fe_{0.125})_2O_4$–5 mol% TiO_2.

1. Introduction

The applications of humidity sensors are widespread, covering domestic electric appliances, automobiles, medical services, various industries and agriculture. The purposes of adopting humidity sensors and the operating conditions are quite different depending on the field of application. In response to this situation, various kinds of humidity sensor have been investigated and developed. The sensing materials are roughly classified into three groups: electrolytes [1–3], organic polymers [4–6] and porous ceramics [7–13]. The porous ceramics are considered excellent in thermal and physicochemical stability compared to devices made by electrolytic or organic polymer materials, and are also feasible for use with integrated circuits.

Based on the well-known fact that the electrical conductivity of metal oxides is affected by surrounding water vapour, many kinds of ceramic have been investigated actively as humidity sensor materials. Ceramic humidity sensors can be classified into two types according to whether the electric conduction is electronic or ionic. Humidity sensors of ionic conduction type have already been developed by using porous ceramics such as $MgCr_2O_4$–TiO_2 [9], TiO_2–V_2O_5 [14], ZnO–Cr_2O_3–Li_2O [15] and so on. In this type, the conductivity is usually enhanced by physisorption or capillary condensation of water at room temperature, and the protons dissociated from water molecules are probably the dominant carrier.

In this paper, a new humidity sensing material composed of $Ni(Al_{1-x}Fe_x)_2O_4$–TiO_2 ceramic is investigated. Certain compositions in this system exhibit an extremely high humidity-sensitive effect, a short response time, and very small hysteresis. The microstructure and humidity-sensitive properties of this ceramic humidity sensor system are reported.

2. Experimental procedure

For the raw materials, reagent-grade NiO, Al_2O_3, Fe_2O_3 and TiO_2 were used. The raw materials were weighed in the molar proportion of $Ni(Al_{1-x}Fe_x)_2O_4$–$yTiO_2$ for $x = 0$, 0.125, 0.25, 0.375, 0.50, 0.625, 0.75, 0.875 and 1 and for $y = 5$, 10, 15 and 20 mol% (Table I). The raw materials were mixed in a ball mill with pure water as a mixing medium. After the water was evaporated, the mixed powder was calcined at 1000 °C for 3 h. The calcined powder was ground with water in a ball mill, then dried and granulated. The granulated powder was pressed into a disc of 10 mm diameter and sintered in air at 1200 to 1350 °C for 3 h. The ceramic body after sintering was lapped to 0.25 mm thickness. After that, porous RuO_2 electrodes were applied to opposite surfaces of the lapped ceramic body by printing and firing.

The crystalline phases of the ceramic body were identified by powder X-ray diffraction (XRD) with CuK_α radiation, and the microstructure was observed by SEM. The porosity of these ceramics was measured by mercury penetration porosimetry.

Relative humidity (RH)–resistance characteristics were measured by a conventional multimeter and HP4192A Impedance Analyser. Relative humidities ranging from 20 to 90% RH, were supplied by an environment testing chamber. The response time and sensitivity were examined by recording the resistance changes when the relative humidity varied from 31 to 91% RH and from 91 to 31% RH.

3. Results and discussion

XRD analysis shows that up to 20 mol% TiO_2, the compositions with high Al contents are single-phase with a pure spinel structure. For high Fe contents, however, the compositions with TiO_2 more than 5 mol% consist of a spinel phase and an $NiTiO_3$ phase. The lattice constant of the system changes from 0.8048 nm ($NiAl_2O_4$) to 0.8339 nm ($NiFe_2O_4$).

The microstructures were examined using SEM. As shown in Fig. 1, each composition is characterized by a typical porous structure. As would be expected from the pore structure, the grains are interconnected by

0022–2461/91 $03.00 + .12

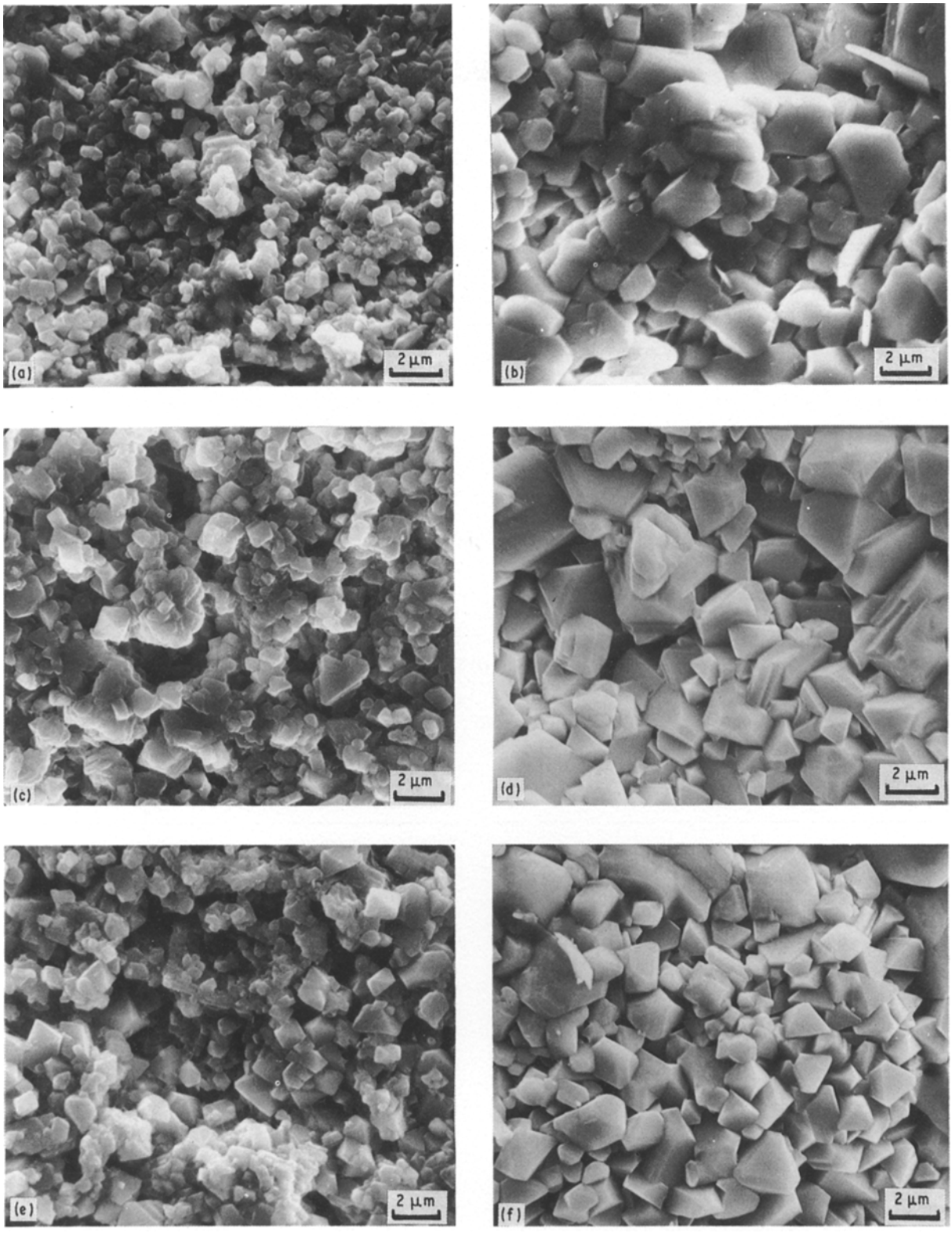

Figure 1 SEM of sintered samples: (a) A-1, (b) A-4, (c) E-1, (d) E-4, (e) I-1, (f) I-4.

necks. The average grain size increases and the ratio of small to large pores decreases with an increase of TiO_2, as in the case of $MgCr_2O_4$–TiO_2 ceramics [9]. Table II gives the porosity of each composition at different sintering temperatures. The porosity decreases slightly when TiO_2 is added. For the same composition, the porosity decreases with increasing sintering temperature.

It is well known that water molecules exhibit chemisorption as well as physisorption on an oxide surface, but the physisorption of water molecules has a decisive role in ceramic humidity sensors [12]. Fig. 2 shows the relative humidity–resistance characteristics of the system; the resistance of the element decreased exponentially with an increase in relative humidity. From the results of this figure, it is found that the resistance of the system decreases with increasing amount of Fe. This phenomenon can be explained as follows. The total resistance of the ceramic body is expressed by summing the intrinsic resistance of the

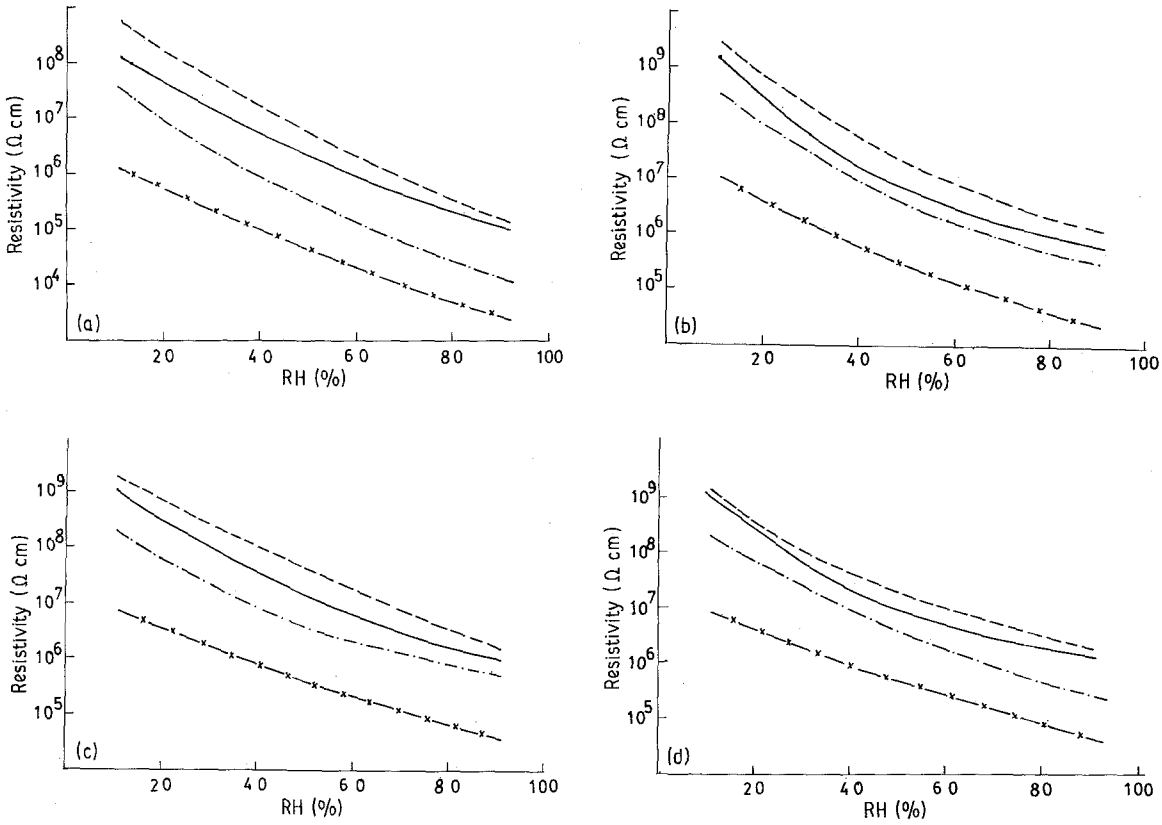

Figure 2 The resistivity–humidity characteristics of the system with (a) 5, (b) 10, (c) 15 and (d) 20 mol % TiO_2: (——) A composition, (– –) B composition, (–·–) E composition, (–×–) H composition.

TABLE I Composition of the $Ni(Al_{1-x}Fe_x)_2O_4$–$yTiO_2$ system under study

	y (mol %)			
x	5	10	15	20
0	A-1	A-2	A-3	A-4
0.125	B-1	B-2	B-3	B-4
0.250	C-1	C-2	C-3	C-4
0.375	D-1	D-2	D-3	D-4
0.500	E-1	E-2	E-3	E-4
0.625	F-1	F-2	F-3	F-4
0.750	G-1	G-2	G-3	G-4
0.875	H-1	H-2	H-3	H-4
1	I-1	I-2	I-3	I-4

element in a dry environment and the resistance of the condensed water in the pores [16]. The variation of intrinsic resistance with composition can be explained by the controlled-valency theory [17]. The low electrical resistivity of high Fe-content compositions is related to the random location of Fe^{2+} and Fe^{3+} ions on the octahedral sites of the spinel structure, so that electron transfer from cation to cation can take place, but the number of electron transfers is decreased with increasing amounts of Al, so the resistance is higher for high-Al compositions.

Table III shows the relationship between the sensitivity (3–91% RH) and the composition, all the samples being sintered at the same temperature. From this table it is found that the sensitivity decreases with increasing amounts of Fe and Ti. From the microstructure analysis, it is found that the porosity is

TABLE II Porosity (%) of the system for different sintering temperatures

Samples	Sintering temperature (°C)	TiO_2 (mol %)			
		5	10	15	20
A	1230	35.8	32.9	32.7	30.5
	1280	32.7	30.5	29.3	30.2
	1330	30.7	25.1	20.9	20.8
B	1230	36.3	32.1	27.9	23.6
	1280	35.1	29.2	25.6	24.3
	1330	33.1	32.3	24.8	20.2
C	1230	33.4	28.9	21.2	20.1
	1280	30.4	22.4	19.8	17.7
	1330	31.6	21.7	19.3	19.0
D	1230	32.1	23.6	26.1	19.2
	1280	32.5	23.2	24.6	18.4
	1330	29.0	27.5	19.7	17.6
E	1230	32.4	28.7	28.2	20.4
	1280	31.8	27.9	28.5	21.6
	1330	29.1	27.4	22.2	18.2
F	1230	30.1	24.2	23.1	22.6
	1280	28.2	27.3	27.1	23.4
	1330	25.9	24.7	20.6	16.2
G	1230	27.6	25.3	23.6	23.1
	1280	28.9	24.3	22.2	21.7
	1330	25.3	26.4	23.1	18.8
H	1230	26.1	26.7	20.6	19.3
	1280	25.4	24.1	20.8	17.8
	1330	25.6	27.3	23.4	18.4
I	1230	23.7	19.3	19.0	18.8
	1280	22.5	18.9	16.2	18.3
	1330	21.3	20.4	19.1	15.4

TABLE III Sensitivity of the $Ni(Al_{1-x}Fe_x)_2O_4$–$yTiO_2$ system with operating temperature at 35 °C

	Sensitivity			
x	$y = 5$ mol %	$y = 10$ mol %	$y = 15$ mol %	$y = 20$ mol %
A	2267	2025	1000	933
B	3000	1967	1313	667
C	1272	755	722	556
D	1016	1046	890	594
E	1238	1000	846	355
F	761	590	262	344
G	852	808	344	181
H	480	524	166	182
I	139	105	122	70

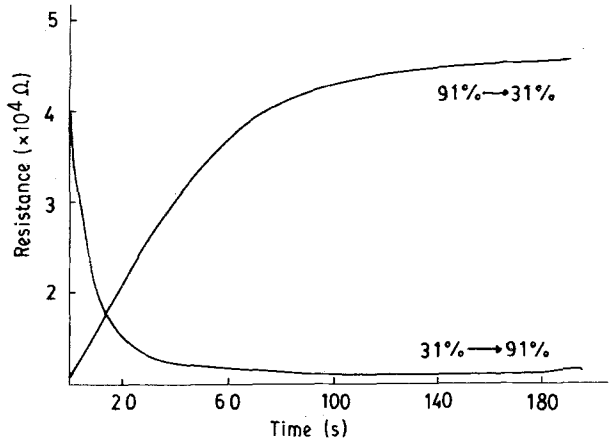

Figure 3 The response curve of the B-1 composition.

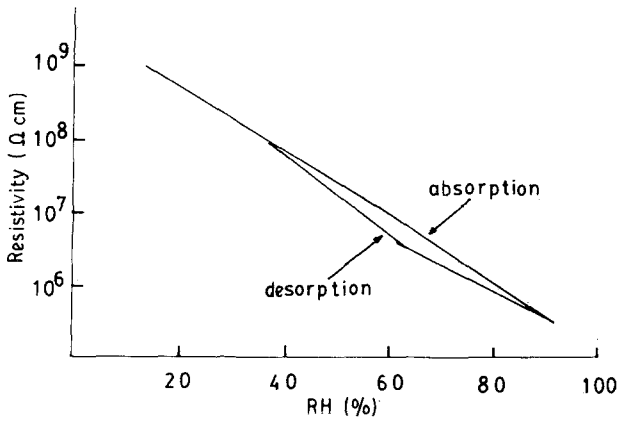

Figure 4 The hysteresis phenomenon of the B-1 composition.

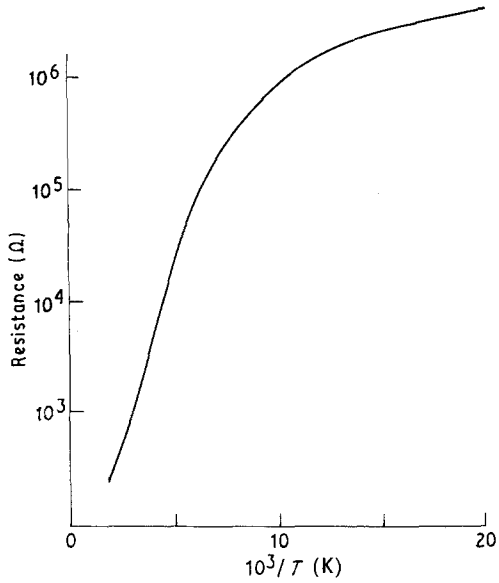

Figure 5 The resistance–temperature relationship of the B-1 composition.

decreased and average grain size increased with an increase of TiO_2. So the surface area of the ceramic and also the volume for capillary condensation are decreased with an increase of TiO_2, and this causes the sensitivity to decrease.

From the results of Seiyama *et al.* [12] it is found that if a specimen has a high resistance, it is difficult to measure the resistance in a low-humidity environment. On the other hand, if it has a low resistance, the humidity dependence becomes relatively too small to be measured conventionally. Therefore, it is desirable that the resistance of the specimen changes exponentially from about 10^7 to $10^4\,\Omega$ as the relative humidity increases from 30 to 90% RH. In this system, we found that the composition B-1 [$Ni(Al_{0.875}Fe_{0.125})_2O_4$–5 mol % TiO_2] had the best sensitivity (Table III) and was very suitable for use as a humidity sensor.

The response curve of the B-1 composition is shown in Fig. 3, with the humidity changed from 31 to 91% RH and from 91 to 31% RH. From this figure, it is found the time required for water vapour absorption is within 20 s. However, when the humidity was reduced the water could not be desorbed immediately, probably due to condensed water filling "ink bottle" pores [16], and the time needed for desorption was longer. Fig. 4 shows the hysteresis phenomenon of the B-1 composition. When a porous ceramic body is exposed to an environment with relative humidity above 40%, capillary condensation of water into a liquid phase may physically occur. As the humidity is reduced, the water cannot desorb immediately and thus causes hysteresis. From Fig. 4 the hysteresis phenomenon occurred when the relative humidity was higher than 40% RH, but it was not found under lower-humidity conditions. The temperature dependence of resistivity of the B-1 composition is shown in Fig. 5; it is found that the sensor ceramic exhibits the typical thermistor property with negative temperature coefficient.

4. Conclusions

In $Ni(Al_{1-x}Fe_x)_2O_4$–$yTiO_2$ ceramic system, for high Al content. Compositions up to 20 mol % TiO_2 are single phase with a pure spinel structure. For high Fe contents, however, compositions with more than 5 mol % TiO_2 consist of a spinel phase and an $NiTiO_3$ phase. The sintered compact shows a typical porous structure, and is suitable for use as a humidity sensor.

The electrical conductivity of the present porous ceramics is enhanced by water absorption. The sensitivity of the system decreases with increasing Fe and Ti. The $Ni(Al_{0.875}Fe_{0.125})_2O_4$–5 mol % TiO_2 composition has the highest sensitivity, short response time for humidity detection (less than 40 s), and high stability.

References

1. F. W. DUNMORE, *J. Res. NBS* **23** (1939) 701.
2. K. NAKAMURA, K. ONO and K. KAWADA, *Electroanal. Chem. Interf. Electrochem.* **47** (1974) 175.
3. J. SHIBA, "Humidity and Moisture" (Korona, Tokyo, 1975) Ch. 2.
4. T. ISHIDA, T. OBAYASHI, K. KUWAHARA and H. HATANAKA, *Nat. Tech. Rept.* **24** (1978) 436.
5. H. ISOGAI and T. WAKABAYASHI, *Instr. Technol.* (1974) 49.
6. G. A. LEE, *Control & Instr.* (1975) 29.
7. T. NITTA and S. HAYAKAWA, *IEEE Trans. Comp. Hyb. Manu. Tech.* CHMT **3** (1980) 237.
8. R. A. MARRA, Y. NAKAMURA, S. FUJITSU and H. YANAGIDA, *J. Amer. Ceram. Soc.* **69** (1986) C-143.
9. T. NITTA, Z. TERADA and S. HAYAKAWA, *ibid.* **63** (1980) 295.
10. T. YAMAMOTO and H. SHIMIZU, *IEEE Trans. Comp. Hyb. Manu. Tech.* **3** (1980) 237.
11. Y. SHIMIZU, M. SHIMABUKURO, H. ARAI and T. SEIYAMA, *Chem. Lett.* (1985) 917.
12. T. SEIYAMA, N. YAMAZOE and H. ARAI, *Sensor & Actuators* **4** (1983) 85.
13. L. WU, C. C. WU and H. M. WU, *J. Electron. Mater.* **19** (1990) 197.
14. K. KATAGAMA, T. AKIBA and H. YANAGIDA, in Proceedings of International Meeting on Chemical Sensors, Fukuoka, Japan, Sept. 19–22, 1983, p. 433.
15. S. UNO, M. HARATA, H. HIRAKI, K. SAKUMA and Y. YOKOMIZO, *ibid.* p. 375.
16. Y. SHIMIZU, H. ARAI and T. SEIYAMA, *Sensors & Actuators* **7** (1985) 11.
17. E. J. VERWEY, *Philips Res. Rep.* **5** (1950) 173.

Received 19 April
and accepted 19 November 1990